http://dx.doi.org/10.5935/0103-5053.20130196

J. Braz. Chem. Soc., Vol. 24, No. 10, 1553-1560, 2013.
Printed in Brazil - ©2013 Sociedade Brasileira de Química
0103 - 5053 $6.00+0.00

Article

Ethanol Oxidation Reaction on IrPtSn/C Electrocatalysts with low Pt Content

Júlio César M. Silva,[a] Beatriz Anea,[a] Rodrigo Fernando B. De Souza,[a] Mônica Helena M. T. Assumpção,[a] Marcelo L. Calegaro,[b] Almir O. Neto[c] and Mauro C. Santos*[,a]

[a]Laboratório de Eletroquímica e Materiais Nanoestruturados (LEMN), Centro de Ciências Naturais e Humanas, Universidade Federal do ABC, Rua Santa Adélia, 166, 09210-170 Santo André-SP, Brazil

[b]Grupo de Materiais Eletroquímicos e Métodos Eletroanalíticos, Instituto de Química de São Carlos, Universidade de São Paulo, CP 780, 13566-590 São Carlos-SP, Brazil

[c]Instituto de Pesquisas Energéticas e Nucleares-Comissão Nacional de Energia Nuclear (IPEN-CNEN), Av. Prof. Lineu Prestes, 2242, 05508-900 São Paulo-SP, Brazil

Neste estudo, a reação de oxidação de etanol (EOR) foi investigada usando materiais nanoestruturados ternários compostos de IrPtSn/C nas proporções em massa Ir:Pt:Sn de 60:30:10, 60:20:20 e 60:10:30, preparados pelo método de precursores poliméricos e comparados com o eletrocatalisador de origem comercial PtSn/C E-TEK. A caracterização por difratometria de raios-X foi utilizada para obter informações acerca da estrutura dos materiais e a microscopia eletrônica de transmissão mostrou que os tamanhos médios das partículas variaram de 5 até 7 nm. A atividade eletrocatalítica foi investigada empregando experimentos cronoamperométricos em 0,5 V *vs.* RHE e através da espectroscopia no infravermelho com transformada de Fourier no modo de refletância total atenuada (FTIR-ATR) *in situ*. Baseado nos experimentos de FTIR-ATR *in situ*, observou-se que o melhor material IrPtSn/C 60:20:20 levou à formação de acetaldeído em altas intensidades e CO_2 em baixas intensidades. Utilizando-se o material IrPtSn/C 60:20:20, foi possível diminuir a quantidade de platina em ca. 73% em comparação com o eletrocatalisador PtSn/C E-TEK, tendo um aumento de ca. 282% na densidade de corrente nos experimentos cronoamperométricos.

In this work, the ethanol oxidation reaction (EOR) was investigated using ternary nanostructured materials composed of IrPtSn/C in mass proportions of Ir:Pt:Sn at 60:30:10, 60:20:20 and 60:10:30, prepared with a polymeric precursor method and compared with commercial electrocatalyst PtSn/C E-TEK. X-ray diffractometry was used to obtain information about the structure of the material. The transmission electron microscopy showed particle sizes of 5-7 nm. The electrocatalytic activity was investigated using chronoamperometry experiments at 0.5 V *vs.* RHE and by *in situ* Fourier transform infrared spectroscopy by attenuated total reflectance (FTIR-ATR) experiments. From *in situ* FTIR-ATR experiments, it can be seen that using the best material IrPtSn/C 60:20:20, the acetaldehyde was produced at high intensities and CO_2 at lower intensities. The use of IrPtSn/C 60:20:20 materials became possible to diminish the Pt fraction to ca. 73% in comparison to the PtSn/C E-TEK electrocatalyst, with an improvement of ca. 282% in the current density of the chronoamperometric experiments.

Keywords: IrPtSn/C, electrocatalysts, ethanol oxidation reaction, FTIR-ATR

Introduction

The use of direct ethanol fuel cells (DEFCs) could offer an excellent alternative solution to the current energy generation problems and could confer major improvements in the prospects for an economy based on renewable energy sources.[1] The use of ethanol is extremely intriguing because ethanol can be obtained from biomass, as in the case of Brazilian sugarcane ethanol. Additionally, ethanol has a high power density and rather low toxicity.[2] However, the high efficiency of the ethanol oxidation reaction (EOR) is still a significant goal because the cleavage of C–C bonds

*e-mail: mauro.santos@ufabc.edu.br

for the complete oxidation of ethanol to CO_2 requires the use of more active and selective anode catalysts.[3-5]

Platinum has been considered as the best chemical element in electrocatalysts for EOR,[6,7] and its electrocatalytic activity can be improved by the addition of other metals, such as Ru,[8-11] Sn,[3,9,11-13] Rh,[1,14] Ce,[15,16] etc. Some studies have indicated that PtSn/C is a promising catalyst for EOR in comparison with other Pt-based binary materials.[3,5,1,17,18] However, a third metal has been added to Pt and Sn with the aim to increase the electrocatalytic activity in EOR. There are many examples of the insertion of a third metal: Cunha *et al.*[19] used ruthenium associated with PtSn/C, while Almeida *et al.*[20] and Ribadeneira *et al.*[21] used nickel with PtSn/C. Additionally, Tayal *et al.*[22] and Ribeiro *et al.*[23] employed iridium with PtSn/C, and all authors obtained a higher activity for EOR in comparison to binary materials, such as PtSn/C.

Cao *et al.*[24] reported that iridium is a promising metal for EOR. The authors obtained better results using Ir_3Sn/C compared to Pt/C and Pt_3Sn/C as the anode in DEFCs, demonstrating the possibility of replacing Pt by Ir in the electrocatalyst. The addition of iridium in the PtSn electrocatalyst can provide oxygen atoms, which promote oxidation of the alcohol residues in a process that can be explained by a bifunctional mechanism.[25] Further, the Ir metal can replace some quantity of platinum in the electrocatalyst for use in ethanol oxidation, according to Silva *et al.*[26] It is also possible that the iridium atoms cause an electronic effect in the orbital symmetries of the PtSn sites.[23] Tayal *et al.*[22] reported that the improvement caused by iridium additions in the PtSn catalyst may be due to the ability of Ir to bind with C. However, Fatih *et al.*[27] reported that because of the high stability of Ir and IrO_2, they are used to stabilize the PtSn/C in acidic solutions in DEFCs.

Aiming to optimize the behavior of the PtSnIr/C electrocatalysts with reductions in the platinum content, this work reports the use of different mass proportions of Pt:Sn:Ir for EOR. The materials were prepared with a polymeric precursor method, and *in situ* FTIR-ATR (Fourier transform infrared spectroscopy by attenuated total reflectance) was used to investigate the EOR results and to determine the product distributions at different potentials as a function of the IrPtSn/C electrocatalyst compositions.

Experimental

Preparation of PtSnIr/C electrocatalysts

The electrocatalyst PtSnIr/C was prepared by the polymeric precursor method.[4,5,26,28] For this purpose, a mass ratio of 1:50:400 (metallic precursor:citric acid (CA):ethylene glycol (EG)) was used to prepare the polymeric resin. Chloroplatinic acid ($H_2PtCl_6 \cdot 6H_20$, 37.5%, Sigma-Aldrich), tin chloride ($SnCl_2 \cdot 2H_20$, 96%, Merck) and iridium chloride ($IrCl_3$, 99.8%, Sigma-Aldrich) were used as the metallic precursors. The prepared polymeric resin was stored under refrigeration. The catalyst was prepared by placing a pre-determined volume of resin in an appropriate amount of carbon Vulcan XC-72R (Cabot Corporation) to give a total metal loading of 20 wt.%. The mixture was homogenized in an ultrasonic bath for 60 min and then thermally treated at 400 °C for 2 h in a N_2 atmosphere.

Material characterization

X-ray diffraction (XRD) analyses were performed with a Rigaku MiniFlex II diffractometer using a Cu K_α radiation source (λ = 0.15406 nm). The diffractograms were recorded from 2θ = 20° to 75° with a step size of 0.02° and a scan rate of 2 s *per* step.[29] Transmission electron microscopy (TEM) was performed using a JEOL JEM 2100 electron microscope operated at 200 kV. Using this setup, the morphologies, distributions and sizes of the nanoparticles were studied by depositing the particles on supports. The mean particle sizes were determined based on measurements of the sizes of 300 randomly chosen particles from different regions in each sample.

Electrocatalyst activity characterization

Electrochemical measurements were performed at room temperature using an Autolab PGSTAT 302N potentiostat. Glassy carbon (GC) electrodes were employed as supports for the working electrodes (0.07 cm^2 of geometric area). In a three-compartment electrochemical cell, a large Pt foil was used as a counter electrode and all potentials were referred to a reversible hydrogen electrode (RHE). Before each experiment, the GC support was polished with an alumina suspension (1 μm) to a mirror finish and was washed in a mixture of ethanol and water. Ultrapure water obtained from a Milli-Q system (Millipore®) was used in all experimental procedures.

The working electrodes were constructed by dispersing 8 mg of the electrocatalyst powder in 1 mL water and mixing for 5 min in an ultrasonic bath. After this step, 20 μL of Nafion® solution (5%) were added to the suspension, and the solution was mixed again in an ultrasonic bath for 15 min. Aliquots of 16 μL of the dispersion fluid were pipetted onto the glassy carbon support surface. Finally, the electrode was dried at 60 °C for 20 min and then was hydrated for 5 min in water.

The *in situ* spectroelectrochemical FTIR-ATR measurements were performed with a Varian® 660 IR spectrometer equipped with a MCT (HgCdTe) detector cooled with liquid N_2, a MIRacle with a Diamond/ZnSe Crystal Plate (Pike®) ATR accessory and a special cell.[5] These experiments were performed at 25 ºC in 0.1 mol L^{-1} $HClO_4$ containing 1.0 mol L^{-1} ethanol. The absorbance spectra were collected as the R/R_0 ratio, where R represents a spectrum at a given potential and R_0 is the spectrum collected at 0.05 V. Positive and negative directional bands represent gain and loss of species at the sampling potential, respectively. The spectra were computed from 128 interferograms averaged from 2500 to 850 cm^{-1} with the spectral resolution set to 4 cm^{-1}. Initially, a reference spectrum (R_0) was measured at 0.05 V, and the sample spectra were collected after applying successive potential steps from 0.2 to 1.0 V.

Results and Discussion

Figure 1 shows the XRD patterns for the IrPtSn/C materials. In this figure, it can be observed that all catalysts have a peak at 25°, which is attributed to the hexagonal structure (002) of the Vulcan XC-72R carbon.[24] Additionally, the peaks at about 27°, 35° and 53° correspond to the tetragonal systems of both SnO_2 and IrO_2. The peak at about 58° correspond to IrO_2. The face-centered cubic systems of Pt and Ir can be identified by peaks at approximately 39°, 46° and 67°.[24]

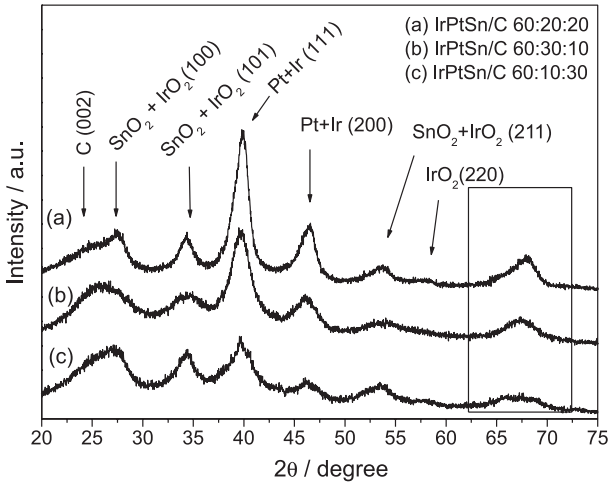

Figure 1. X-ray diffraction patterns for the IrPtSn/C electrocatalysts.

The region at 67°, which is highlighted by a rectangle, exhibits a prominence that increases with increasing Pt fraction. This is because the peaks in this region are related to platinum (220), iridium (220) and iridium oxide (310). To obtain more information regarding these peaks with respect to the lattice and crystallite size parameters, the XRD patterns were refined using the Pawley method[30] carried out with Fityk 0.98 software, as reported by Wojdyr.[31]

In Figure 2, it is possible to observe the change in the peak shape as a result of an increasing platinum fraction. This peak is due to changes in the distribution of crystallographic faces, such as the lower participation

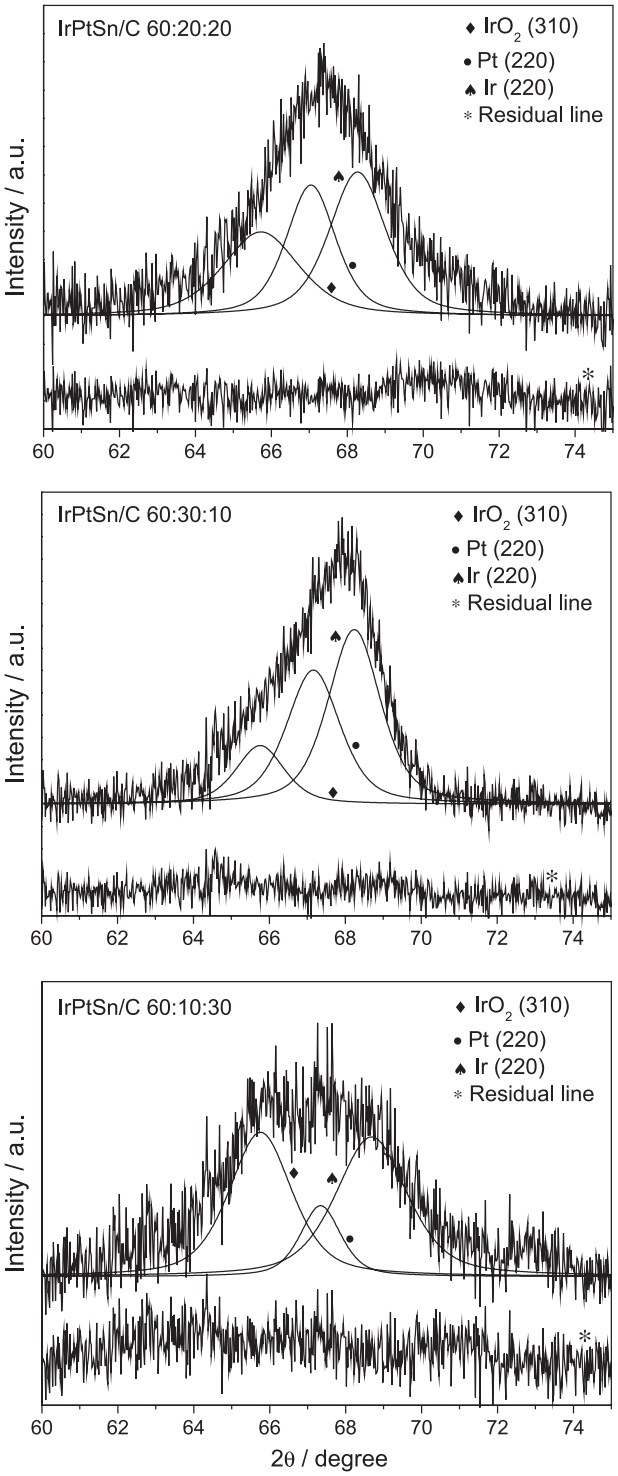

Figure 2. XRD pattern decomposition for IrPtSn/C using the Pawley refinement method.

of the plane (310) of IrO_2 with the simultaneous increase of the peak related to the plane (220) of Pt. In Table 1, the calculated values of the mean crystallite sizes and the lattice parameters for the platinum and iridium faces are presented.

Table 1. XRD results for the IrPtSn/C (60:10:30; 60:20:20; 60:30:10) electrocatalysts

Catalyst composition (Ir:Pt:Sn)	60:10:30	60:20:20	60:30:10
Lattice parameter of Pt / nm	0.393	0.394	0.394
Lattice parameter of Ir / nm	0.389	0.389	0.390
Mean crystallite size of Pt / nm	7	6	6
Mean crystallite size of Ir / nm	5	5	6
Mean crystallite size of IrO2 / nm	5	5	5

It can be seen that the iridium lattice parameter is 0.389 nm, which is very close to that obtained by Cao *et al.* for Ir/C.[24] However, the lattice parameters for Pt for all compositions are shifted toward more positive values (0.393 nm and 0.394 nm) for the material produced than that (0.392 nm) otherwise measured for nanostructured polycrystalline Pt/C,[24] indicating that an expansion of the platinum unit cell has occurred. This suggests that small amounts of Sn atoms can be inserted in Pt crystallite as an alloy, as indicated in other works.[13,23,24,27]

Transmission electron microscopy (TEM) images of IrPtSn/C 60:20:20, IrPtSn/C 60:30:10 and IrPtSn/C 60:10:30 are shown in Figures 3a, 3b and 3c, respectively. These figures show that the nanoparticles are uniformly dispersed on the carbon support. The particle size distributions of the nanoparticles were obtained by measuring the sizes of 300 randomly chosen from various TEM images of each catalyst. Figures 3d, 3e and 3f show the histograms of the catalyst particle mean diameter distribution for IrPtSn/C 60:20:20, IrPtSn/C 60:30:10 and IrPtSn/C 60:10:30, respectively. The particles have average sizes of 6.1 nm for IrPtSn/C 60:20:20, 5.7 nm for IrPtSn/C 60:30:10 and 5.3 nm for IrPtSn/C 60:10:30. It should be noted that 100% of the particles are between 2 and 10 nm in size for all materials studied. These results are in agreement with other literature results in which the precursor polymeric method was utilized for electrocatalyst preparation.[4,5,23,32]

The electrocatalytic activity for the ethanol electrooxidation of IrPtSn/C 60:20:20, IrPtSn/C 60:10:30, IrPtSn/C 60:30:10 and PtSn/C E-TEK 75:25 catalysts at 0.5 V (*vs*. RHE) potential range were obtained from chronoamperometry measurements. The potential was held at 0.5 V for 30 min. In all chronoamperometric curves shown in Figure 4, the current decreases continuously within the first several minutes, and after some time, the fall is less pronounced. However, curves (a) and (b) decrease

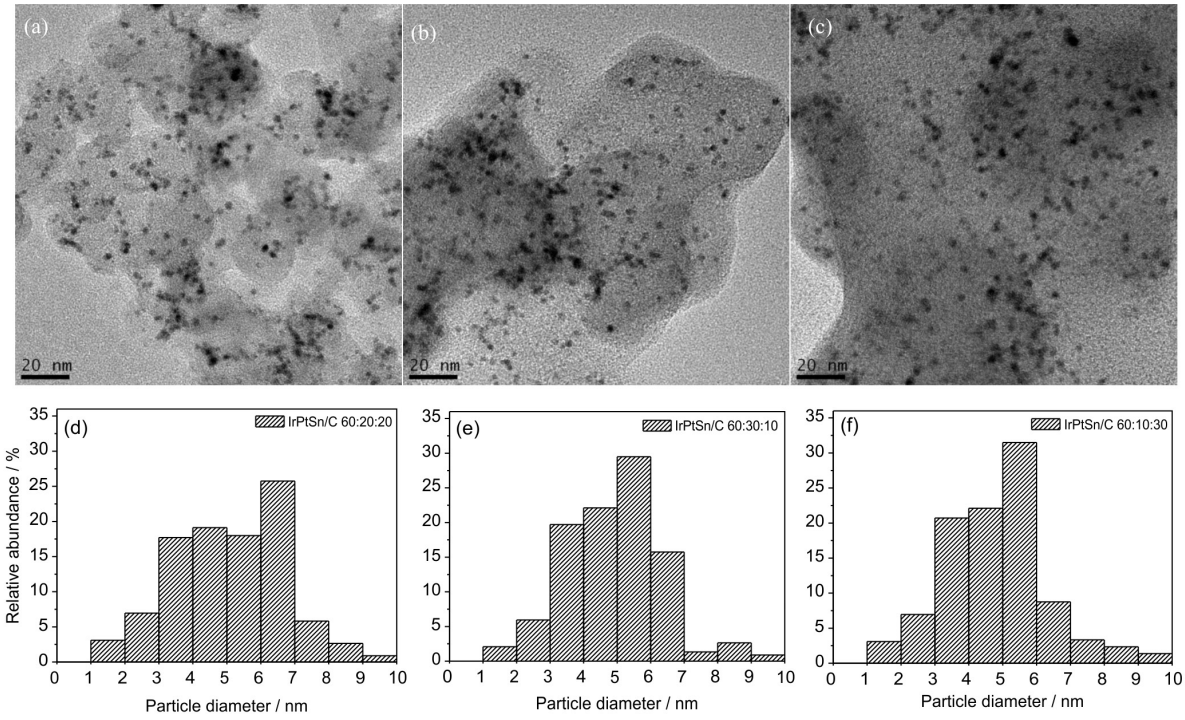

Figure 3. (a) TEM micrograph of the IrPtSn/C 60:20:20 electrocatalyst and (d) histogram of the catalyst particle mean diameter distribution for this electrocatalyst; (b) TEM micrograph of the IrPtSn/C 60:30:10 electrocatalyst and (e) histogram of the catalyst particle mean diameter distribution for this electrocatalyst; (c) TEM micrograph of the IrPtSn/C 60:10:30 electrocatalyst and (f) a histogram of the catalyst particle mean diameter distribution for this electrocatalyst.

relatively more sharply than others. The current value may decay due to poisoning of surface active sites and instability of catalyst particles. These effects decrease slowly the number of active sites and are responsible for the continuous and slow current time decay.[22,23]

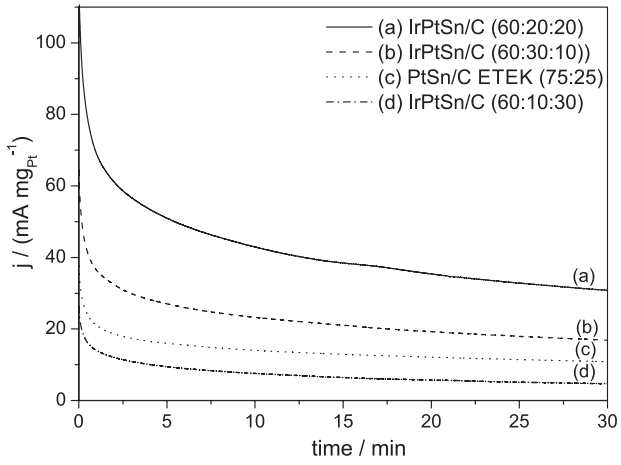

Figure 4. Chronoamperometry curves for the 20 wt.% IrPtSn/C and PtSn/C E-TEK electrocatalysts in 1.0 mol L^{-1} CH_3CH_2OH + 0.5 mol L^{-1} $HClO_4$, E = 0.5 V, time = 30 min and temperature = 25 °C.

The highest current density measured for EOR was obtained using IrPtSn/C (60:20:20). After 30 min, the current was 31 mA mg_{Pt}^{-1}, which is approximately 3 times higher than that observed for PtSn/C E-TEK (11 mA mg_{Pt}^{-1}).

Comparing IrPtSn/C 60:30:10 with IrPtSn/C 60:20:20, it can be observed that, when the percentage of Pt was increased and the Sn decreased, the activity with respect to EOR was reduced. When the Pt amount was decreased to 10% and the Sn increased to 30% (IrPtSn/C 60:10:30), the resulting activity was the worst for all materials. This result is most likely due to the very low amount of platinum present on the electrocatalyst. Using IrPtSn/C 60:20:20 materials as shown in Figure 4, it was possible to diminish the Pt amount to approximately 73% in comparison to the PtSn/C E-TEK electrocatalyst, yielding an improvement of approximately 282% in the current density within the chronoamperometric experiments. This is important since the iridium is approximately 35% cheaper than platinum as recently reported by Brouzgou *et al.*[33]

Many works have reported an optimal composition for each preparation method with respect to either the methanol or ethanol oxidation reaction.[2,27,34,35] This occurs because there are differences between shapes, phases, dispersions, morphologies and superficial phases, and these parameters can contribute either high or low coverage of the adsorption sites within the oxide.[6,7,36] Additionally, it is known that platinum is an excellent metal for hydrogen adsorption,[1,37] and that Sn can form Sn–OH species at lower potentials than platinum.[38,39] Hence, the addition of Ir to the PtSn electrocatalyst can lead to an increase in the oxophilic character of the surface, increasing the Sn–O bond strength and the acidity of the Sn–OH sites, which also can favor ethanol electrooxidation at lower potentials.[23] Another possibility is that the iridium atoms cause a disturbance at the PtSn sites and in the orbital symmetries, thereby affecting the orbital spatial distribution, the ethanol adsorption and, consequently, the electrooxidation rate.[23] Tayal *et al.*[22] reported that improvements gained by iridium addition into the PtSn catalyst may be due to the ability of Ir to bind C. We suggest that the best result obtained with the IrPtSn/C 60:20:20 material was due to the presence of an enhanced synergic effect for this specific metal ratio, and the combination of various contributions of different properties of distinct phases and/or metals in this ratio led to an improvement in the electrocatalytic activity for the ethanol oxidation reaction. Additionally, it is known that the strongest effect of the bifunctional mechanism depends on achievement of the best ratio between the metals.[10,40] Hence, the same happens for the electronic effect on Pt-based materials, which may decrease the activation energy for global ethanol oxidation reaction.[41-43] Therefore, the beneficial synergistic effect between Sn and Ir with Pt in addition to the optimal composition of IrPtSn/C can be used to improve the ethanol oxidation reaction.[22]

To better understand the results of ethanol electrooxidation, *in situ* FTIR-ATR was used to study the ethanol oxidation reaction pathways and to determine the product distributions at different potentials.

Figure 5 shows the sets of spectra measured for EOR on the IrPtSn/C 60:10:30, IrPtSn/C 60:30:10 and IrPtSn/C 60:20:20 electrocatalysts. In these spectra, the bands related to acetic acid (1282 cm^{-1}),[44] acetaldehyde (933 cm^{-1})[1] and CO_2 (2343 cm^{-1})[45] can be observed.

In Figure 5, an additional three intense bands are present, corresponding to the main reaction products and the intermediates. The first appears at approximately 1130 cm^{-1} and corresponds to perchloric acid, while the other two bands are between 1640-1750 cm^{-1} and were attributed to the vibrations of two different species, including the interfacial water (1640 cm^{-1}) and the acetaldehyde and/or acetic acid (stretching mode νCO from the carbonyl group at approximately 1720 cm^{-1}).[41]

The high interference of the water band could be caused by the large amount of iridium in the PtSn electrocatalysts, thereby leading to an increase in the oxophilic character of the surface, increasing the Sn–O bond strength and the acidity of the Sn–OH sites. Ultimately, this would lead to the adsorption of a significant amount of water at the electrode surface.[23]

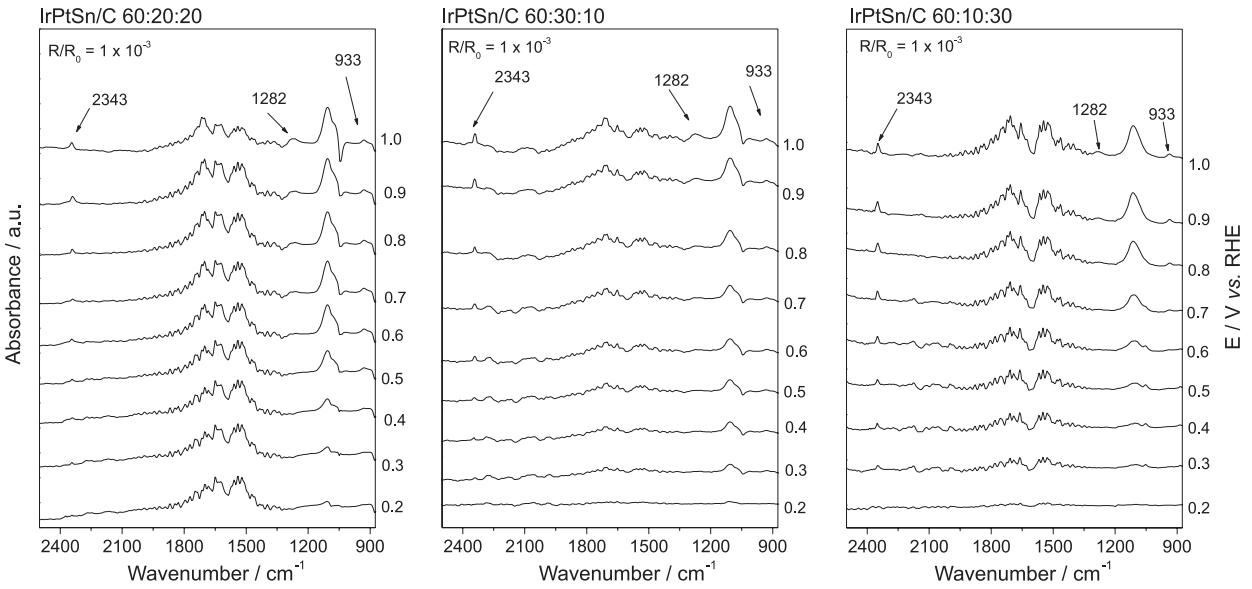

Figure 5. *In situ* FTIR-ATR spectra obtained from 0.2 to 1.0 V (RHE) in 0.1 mol L^{-1} $HClO_4$ + 1.0 mol L^{-1} ethanol using IrPtSn/C electrocatalysts.

To evaluate the effects of the catalyst structures on the product distribution during EOR at different potentials, all bands were deconvoluted by Lorentzian line forms.[4,5] Thus, the intensity and line width of each band can be analyzed individually. The integrated intensities of the acetic acid, acetaldehyde and CO_2 bands were normalized for the intensity obtained at 1.0 V, as described by Lima *et al*.[46] The results are shown in Figure 6.

Analyzing Figure 6a in which the relative intensities of acetaldehyde are presented for all materials studied, it can be observed that, at 0.5 V (at the same potential that was used for the chronoamperometric experiments), acetaldehyde yields the highest intensity in the IrPtSn/C 60:20:20 material. Hence, using this electrocatalyst, a higher current density for EOR was obtained. When the IrPtSn /C 60:10:30 material was used, the acetaldehyde reached the lowest intensity, resulting in the worst result for EOR. Based on this figure, it is also possible to observe that, when using IrPtSn/C 60:10:30, the acetaldehyde intensity is very low until 0.5 V. However, when the 60:20:20 and 60:30:10 proportions are incorporated into the analysis, the intensity of the acetaldehyde band is relatively high for the low potentials.

Observing Figure 6b, it is possible to note the relative intensities of acetic acid. At 0.5 V, this product gives the highest intensity when IrPtSn/C 60:30:10 was the material

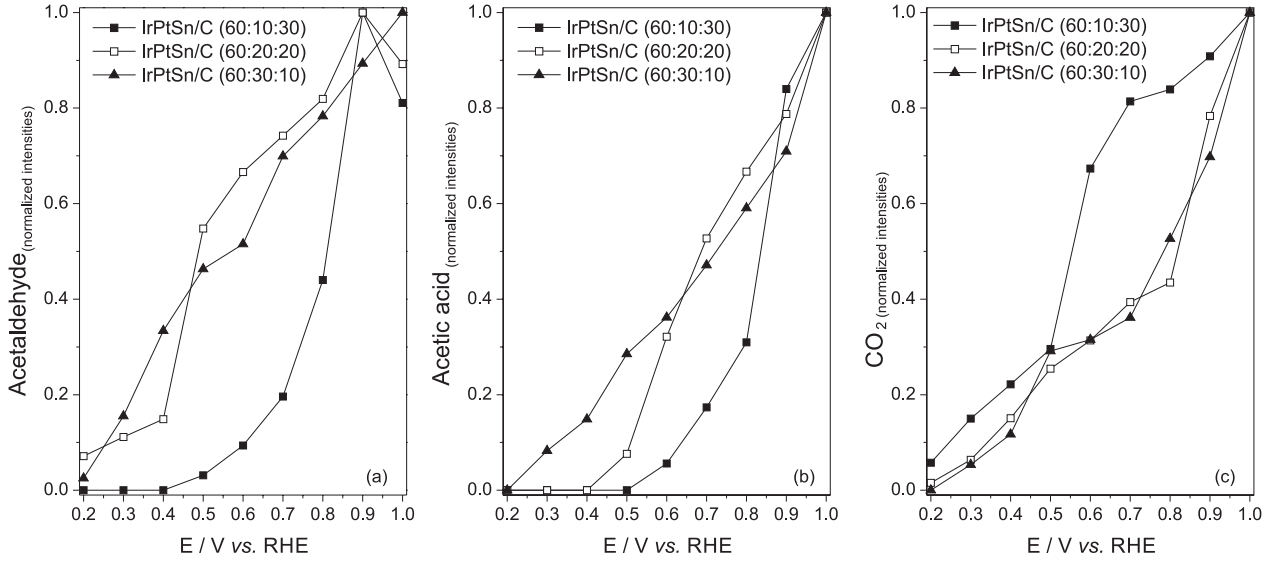

Figure 6. The integrated intensities of the bands of acetaldehyde, acetic acid and CO_2 as functions of the potential for IrPtSn/C 60:20:20, IrPtSn/C 60:30:10 and IrPtSn/C 60:10:30.

utilized, whereas when the material was IrPtSn/C 60:10:30, the intensity of this product was approximately zero. Additionally, when IrPtSn/C 60:20:20 was used, the acetic acid intensity was considerably lower in comparison to that of IrPtSn/C 60:30:10. It also can be seen that the acetic acid was produced in low potential when IrPtSn/C 60:30:10 was used. This is probably because this material has higher amount of platinum than others. Therefore, more sites for ethanol adsorption, and taking into account that in this material IrO_2 and SnO_2 are present, water can be activated at low potentials.[22,24] For this reason, some intermediate of adsorbed ethanol could be oxidized directly to acetic acid[14,40] in low potentials.

Figure 6c presents the relative intensities of CO_2. Based on this figure, it can be observed that at 0.5 V, the CO_2 the increasing tendency of the CO_2 signal is similar for all of the materials, although with respect to IrPtSn/C 60:20:20, this intensity is slightly smaller. An important fact is that in all potentials range, except at 0.5 V and 1.0 V, the CO_2 intensity is the highest using IrPtSn/C 60:10:30 compared to other two materials.

Additionally, it is possible to compare the results obtained here for ethanol oxidation using the PtSnIr/C materials against those obtained using PtSn/C E-TEK for the same process, as published in our recent work.[4] In this case, the latter catalyst displays a higher intensity of CO_2 in all potential regions compared to that of acetic acid and acetaldehyde.

Based on these results, the best electrocatalytic activity was obtained for the ethanol oxidation reaction using IrPtSn/C 60:20:20, which may be associated with an increased production of acetaldehyde and a reduced production of CO_2. Silva *et al.*[5] carried out the EOR experiments with *in situ* FTIR-ATR investigation using alloyed and non-alloyed PtSn/C. They observed that an increased amount of CO_2 was produced from the material for which the worst EOR current density was produced. Additionally, the authors reported slow kinetics for the CO_2 formation.[5] Ziagnani *et al.*[47] studied different compositions of Pt:Sn as anodes in a DEFC. Using high performance liquid chromatography, the authors determined that the best material led to reduced amounts of CO_2 (at 70 °C) and increased amounts of acetic acid, which could be one of the factors causing the increased electrocatalytic activity of the IrPtSn/C 60:20:20 material. This is because with this material, reduced formation of CO_2 was obtained. Another contributor could be the fact that the kinetics of acetaldehyde formation may be enhanced using the IrPtSn/C 60:20:20 material.

The results obtained with IrPtSn/C electrocatalysts are in agreement with those published by other authors. Tayal *et al.*[22] used gas chromatography to analyze the liquid products formed due to ethanol electrooxidation at different compositions of PtIrSn/C. However, the authors did not use iridium at higher concentrations for any material composition. Based on the results presented by this author, it can be observed that the increase in the relative amount of iridium causes an increase in the acetaldehyde formation, as well. This indicates that iridium led to the formation of acetaldehyde as the principal product resulting from the ethanol oxidation reaction. Using IrPtSn/C 60:10:30, acetaldehyde was observed at a low intensity, while CO_2 was observed at a higher intensity. This is most likely due to the large amount of Sn used in this proportion. In the work by Ziagnani *et al.*,[47] it is possible to observe that the increase in the Sn content in the PtSn/C electrocatalyst caused the decrease in the acetaldehyde production.

Therefore, for the IrPtSn/C electrocatalysts with high amounts of iridium and low amounts of Sn, acetaldehyde is the product of highest intensity, and if the amount of Sn is increased, the CO_2 is formed at higher intensities.

Conclusions

Based on the results presented in this study, IrPtSn/C 60:20:20 is the optimal proportion for the ethanol oxidation reaction. Using this material, it was possible to decrease the Pt fraction to approximately 73% in comparison to the PtSn/C E-TEK electrocatalyst, yielding an improvement of approximately 282% of the current density in chronoamperometric experiments. *In situ* FTIR-ATR analysis of the ethanol oxidation reaction demonstrated that acetaldehyde was the product yielded in highest intensities. This is likely due to the high amount of iridium and low amount of tin in this proportion because the iridium led the ethanol oxidation reaction to produce acetaldehyde, while higher amounts of Sn led to acetic acid formation.

Acknowledgments

The authors wish to thank the Brazilian funding institutions CNPq (Process No. 474732/2008-8), CAPES, FAPESP (Processes No. 05/59992-6, 09/09145-6, 10/07831-7 and 10/16511-6), Instituto Nacional de Ciência e Tecnologia (INCT) de Energia e Meio Ambiente (Process No. 573.783/2008-0) and UFABC for their financial support.

References

1. Li, M.; Kowal, A.; Sasaki, K.; Marinkovic, N.; Su, D.; Korach, E.; Liu, P.; Adzic, R. R.; *Electrochim. Acta* **2010**, *55*, 4331.

2. Godoi, D. R. M.; Perez, J.; Villullas, H. M.; *J. Phys. Chem. C* **2009**, *113*, 8518.
3. Silva, J. C. M.; De Souza, R. F. B.; Parreira, L. S.; Neto, E. T.; Calegaro, M. L.; Santos, M. C.; *Appl Catal., B* **2010**, *99*, 265.
4. De Souza, R. F. B.; Parreira, L. S.; Silva, J. C. M.; Simões, F. C.; Calegaro, M. L.; Giz, M. J.; Camara, G. A.; Neto, A. O.; Santos, M. C.; *Int. J. Hydrogen Energy* **2011**, *36*, 11519.
5. Silva, J. C. M.; Parreira, L. S.; De Souza, R. F. B.; Calegaro, M. L.; Spinacé, E. V.; Neto, A. O.; Santos, M. C.; *Appl. Catal., B* **2011**, *110*, 141.
6. Qian, Q.-Y.; Yang, C.; Zhou, Y.-G.; Yang, S.; Xia, X.-H.; *J. Electroanal. Chem.* **2011**, 660, 57.
7. Liu, C. W.; Chang, Y. W.; Wei, Y. C.; Wang, K. W., *Electrochim. Acta* **2011**, *56*, 2574.
8. Giz, M. J.; Camara, G. A.; Maia, G.; *Electrochem. Commun.* **2009**, *11*, 1586.
9. Wang, H.; Jusys, Z.; Behm, R. J.; *J. Power Sources* **2006**, *154*, 351.
10. Camara, G. A.; de Lima, R. B.; Iwasita, T.; *Electrochem. Commun.* **2004**, *6*, 812.
11. Colmati, F.; Antolini, E.; Gonzalez, E. R.; *J. Power Sources* **2006**, *157*, 98.
12. Zhou, W. J.; Li, W. Z.; Song, S. Q.; Zhou, Z. H.; Jiang, L. H.; Sun, G. Q.; Xin, Q.; *J. Power Sources* **2004**, *131*, 217.
13. De Souza, R. F. B.; Parreira, L. S.; Rascio, D. C.; Silva, J. C. M.; Teixeira-Neto, E.; Calegaro, M. L.; Spinace, E. V.; Neto, A. O.; Santos, M. C.; *J. Power Sources* **2010**, *195*, 1589.
14. Kowal, A.; Gojkovic, S. L.; Lee, K. S.; Olszewski, P.; Sung, Y. E.; *Electrochem. Commun.* **2009**, *11*, 724.
15. De Souza, R. F. B.; Flausino, A. E. A.; Rascio, D. C.; Oliveira, R. T. S.; Neto, E. T.; Calegaro, M. L.; Santos, M. C.; *Appl. Catal., B* **2009**, *91*, 516.
16. Wang, J.; Xi, J.; Bai, Y.; Shen, Y.; Sun, J.; Chen, L.; Zhu, W.; Qiu, X.; *J. Power Sources* **2007**, *164*, 555.
17. Antolini, E.; *J. Power Sources* **2007**, *170*, 1.
18. Zhou, W.; Zhou, Z.; Song, S.; Li, W.; Sun, G.; Tsiakaras, P.; Xin, Q.; *Appl. Catal., B* **2003**, *46*, 273.
19. Cunha, E. M.; Ribeiro, J.; Kokoh, K. B.; de Andrade, A. R.; *Int. J. Hydrogen Energy* **2011**, *36*, 11034.
20. Almeida, T. S.; Kokoh, K. B.; De Andrade, A. R.; *Int. J. Hydrogen Energy* **2011**, *36*, 3803.
21. Ribadeneira, E.; Hoyos, B. A.; *J. Power Sources* **2008**, *180*, 238.
22. Tayal, J.; Rawat, B.; Basu, S.; *Int. J. Hydrogen Energy* **2011**, *36*, 14884.
23. Ribeiro, J.; dos Anjos, D. M.; Kokoh, K. B.; Coutanceau, C.; Léger, J. M.; Olivi, P.; de Andrade, A. R.; Tremiliosi-Filho, G.; *Electrochim. Acta* **2007**, *52*, 6997.
24. Cao, L.; Sun, G.; Li, H.; Xin, Q.; *Electrochem. Commun.* **2007**, *9*, 2541.
25. Ramos, S. G.; Calafiore, A.; Bonesi, A. R.; Triaca, W. E.; Castro Luna, A. M.; Moreno, M. S.; Zampieri, G.; Bengio, S.; *Int. J. Hydrogen Energy* **2012**, *37*, 14849.
26. Silva, J. C. M.; De Souza, R. F. B.; Romano, M. A.; D'Villa-Silva, M.; Calegaro, M. L.; Hammer, P.; Neto, A. O.; Santos, M. C.; *J. Braz. Chem. Soc.* **2012**, *23*, 1146.
27. Fatih, K.; Neburchilov, V.; Alzate, V.; Neagu, R.; Wang, H.; *Acta Mater* **2010**, *195*, 7168.
28. Parreira, L. S.; Silva, J. C. M.; D'Villa-Silva, M.; Simões, F. C.; Garcia, S.; Gauber, I.; Cordeiro, A. M. L.; Leite, L. R.; Santos, M. C.; *Electrochim. Acta* **2013**, *96*, 243.
29. Piasentin, R. M.; Spinace, E. V.; Tusi, M. M.; Neto, A. O.; *Int. J. Electrochem. Sci.* **2011**, *6*, 2255.
30. Pawley, G. S.; *J. Appl. Crystallogr.* **1981**, *14*, 357.
31. Wojdyr, M.; *J. Appl. Crystallogr.* **2010**, *43*, 1126.
32. Purgato, F. L. S.; Olivi, P.; Léger, J. M.; de Andrade, A. R.; Tremiliosi-Filho, G.; Gonzalez, E. R.; Lamy, C.; Kokoh, K. B.; *J. Electroanal. Chem.* **2009**, *628*, 81.
33. Brouzgou, A.; Song, S. Q.; Tsiakaras, P.; *Appl. Catal., B* **2012**, *127*, 371.
34. Eguiluz, K. I. B.; Salazar-Banda, G. R.; Miwa, D.; Machado, S. A. S.; Avaca, L. A.; *J. Power Sources* **2008**, *179*, 42.
35. Neburchilov, V.; Wang, H.; Zhang, J.; *Electrochem. Commun.* **2007**, *9*, 1788.
36. Han, S.-B.; Song, Y.-J.; Lee, J.-M.; Kim, J.-Y.; Park, K.-W.; *Electrochem. Commun.* **2008**, *10*, 1044.
37. Godoi, D. R. M.; Perez, J.; Villullas, H. M.; *J. Power Sources* **2010**, *195*, 3394.
38. Sen Gupta, S.; Singh, S.; Datta, J.; *Mater. Chem. Phys.* **2010**, *120*, 682.
39. Lim, D.-H.; Choi, D.-H.; Lee, W.-D.; Lee, H.-I.; *Appl. Catal., B* **2009**, *89*, 484.
40. Camara, G. A.; de Lima, R. B.; Iwasita, T.; *J. Electroanal. Chem.* **2005**, *585*, 128.
41. Simões, F. C.; dos Anjos, D. M.; Vigier, F.; Léger, J. M.; Hahn, F.; Coutanceau, C.; Gonzalez, E. R.; *J. Power Sources* **2007**, *167*, 1.
42. Batista, E. A.; Malpass, G. R. P.; Motheo, A. J.; Iwasita, T.; *J. Electroanal. Chemistry* **2004**, *571*, 273.
43. Léger, J. M.; *Electrochim. Acta* **2005**, *50*, 3123.
44. Léger, J. M.; Rousseau, S.; Coutanceau, C.; Hahn, F.; Lamy, C.; *Electrochim. Acta* **2005**, *50*, 5118.
45. Camara, G. A.; Iwasita, T.; *J. Electroanal. Chem.* **2005**, *578*, 315.
46. Lima, F. H. B.; Gonzalez, E. R.; *Electrochim. Acta* **2008**, *53*, 2963.
47. Ziagnani, S. C.; Baglio, V.; Linares, J. J.; Monforte, G.; Gonzalez, E. R.; Aricò, A. S.; *Electrochim. Acta* **2012**, *70*, 255.

Submitted: May 7, 2013
Published online: August 20, 2013

FAPESP has sponsored the publication of this article.